# BEATING CILIA IDENTIFICATION IN FLUORESCENCE MICROSCOPE IMAGES FOR ACCURATE CBF MEASUREMENT

*Fan Zhang*[1], *Weidong Cai*[1], *Yang Song*[1], *Paul Young*[2,3], *Daniela Traini*[2,3], *Lucy Morgan*[4,5], *Hui-Xin Ong*[2,3], *Lachlan Buddle*[4], *Dagan Feng*[1]

[1] BMIT Research Group, School of IT, University of Sydney, Australia
[2]Woolcock Institute of Medical Research, Australia
[3]Discipline of Pharmacology, Sydney Medical School, University of Sydney, Australia
[4]Department of Respiratory Medicine, Concord Repatriation General Hospital, Australia
[5]School of Medicine, University of Sydney, Australia

## ABSTRACT

Ciliary beating frequency (CBF) is a regulated quantitative measurement to describe ciliary beating properties. It is widely used for diagnosis of defective mucociliary clearance diseases. Image-based methods can be effective for CBF estimation but also affected by the moving objects such as ciliated cells and debris. In this work, we propose a CBF estimation method by removing these unfavorable objects, which we refer to as foreground, so that we can focus on observing the beating cilia only. We firstly design a graph-based method to divide the cilia image into different regions. Next, the foreground regions are extracted and removed from the region division result. The beating cilia are then recognized from the background and used to compute the CBF. Our method conducts the CBF estimation by incorporating the cilia regions only and thus can provide a more accurate description of ciliary beating properties. Preliminary experimental results on cilia images showed the proposed method's potentials for accurate CBF measurement.

***Index Terms***— Beating cilia, mucociliary clearance, image-based CBF estimation, frequency thresholding

## 1. INTRODUCTION

Mucociliary clearance is the fundamental defensive mechanism for clearing inhaled micro-organisms and environmental particulates in respiratory tract [1, 2]. The coordinated beating of cilia plays an important role in mucociliary clearance by propelling mucus and the trapped debris out of the airways. Ciliary beating frequency (CBF) is a measurable and tightly regulated function for describing the ciliary beating properties, and has proven to be useful for diagnostics and therapy of the defective mucociliary clearance diseases [3, 4].

Although the measurement of CBF has been performed for many years, it remains a challenging task to compute the CBF accurately. The recent approaches process the photoelectric signals obtained with techniques, such as photomultipliers [5] and photodiodes [6], to detect the changes in light intensity passing through the beating cilia [7]. These methods estimate the CBF indirectly using the transmitted or reflected light, instead of making direct use of microscopic images. Thus, the CBF estimation can be very sensitive to the lighting changes. Digital high speed imaging (DHSI) based approach is considered to bring more accurate CBF estimation by recording the actual ciliary beating and enabling the frame-by-frame observation [8, 9]. Manual observation by playing the images in a slow speed is usually more accurate but suffers from issues such as large time consumption, varying observer expertise and fatigue.

More recently, there have been methods that calculate CBF by applying a Fast Fourier Transform (FFT) method on the temporal signals, e.g., intensity variations, of the regions of interest (ROIs) above the cilia [10, 11]. Although these methods avoid the frame-by-frame observation, they require the observer to accurately locate the beating cilia. It is more preferable to recognize them automatically. For example, the whole field analysis from Sission et al. [1] and the harmonic analysis from Koniar et al. [12] tried to recognize the cilia by differentiating the frequency spectrums of different objects based on the idea that the beating cilia have their own spectrums. However, their performance can be affected if the frequency spectrums of the objects are overlapping. For instance, the ciliated cell where the cilia are closely packed sometimes beats simultaneously and may obscure the observation of cilia. In the works from Parrilla and Zhang et al. [13, 14], a moving cell rotation correction is incorporated before the CBF estimation. While these methods can reduce the influence of moving cells for better estimation, we expect further improvement by removing the unfavorable regions.

Therefore, in this study, we propose a method for CBF measurement by removing the ciliated cell and floating debris so that we can identify the frequencies from the beating cilia. A graph-based method is designed to divide the cilia image

into regions, from which the cell and debris are recognized as the foreground and removed. The frequency distribution from the background regions is then used for the CBF estimation. After removing the cell and debris, we could obtain the frequency spectrum from the beating cilia only, which leads to more accurate measurement of CBF.

## 2. METHODS

### 2.1. Image Acquisition

Cilia images, as shown in Fig.1a, were acquired from the sampling of primary ciliated epithelial cells via nasal brushing from 5 healthy, young volunteers at Concord Repatriation General Hospital, Sydney, Australia. For each volunteer, we collected several sample cells and stimulated them with $\beta$-agonist, salbutamol sulfate (SS) and the sugar alcohol, mannitol (MA) at different concentrations and combinations within a 24-hour period. The cells were then mounted onto the stage of an Olympus IX70 fluorescence microscope, connected with a Nikon D7100 camera that records the images at a rate of 60 frames per second and resolution of $720 \times 1280$. 30 cases with the mentioned drugs were used in the experiments, and for each case, we used 300 consecutive images to compute the frequency of each pixel with the FFT method for the frequency map computation.

### 2.2. Region Division

The first step of our method is to divide the cilia image that contains various objects, including the cilia, cells, debris and the culture medium, into different regions. We refer to the unfavorable regions that can affect the measurement of CBF, e.g., the cell and debris, as the foreground regions, and consider the remaining parts with the cilia and culture medium as the background regions. The cilia can be differentiated from the still medium based on the frequency spectrum to compute the CBF with the beating cilia only. A graph-based method is proposed for the region division as illustrated in Fig. 1.

#### *2.2.1. Feature Extraction and Neighbourhood Construction*

Features are extracted from the images to describe the pixels numerically and further to construct the pixel adjacency matrix. We first compute the beating frequency for each pixel to create the frequency map [1]. Then, we calculate the first order texture features, including mean, variance, skewness and kurtosis from a local patch around the pixel. Along with the intensity, each pixel $p$ is represented as a 6-dimensional feature vector $V(p)$. While the frequency describes the different moving behaviours of the objects, the texture features provide the visual differences.

A pixel adjacency matrix $PM$ is then constructed to represent the neighbourhood information, with $pm(p_i, p_j) = 1$ indicating the two pixels are neighbours, otherwise 0. Cosine similarity is applied to calculate the similarity between pixels based on their feature vectors, and the threshold $s_{low}$ is used to regulate the size of neighbourhood for pixel $p_i$, as:

$$pm(p_i, p_j) = 1, \textbf{if } cos(V(p_i), V(p_j)) > S_{low} \quad (1)$$

where $p_j$ belongs to the local patch surrounding $p_i$.

In our experiments, a $5 \times 5$ window with the target pixel at the center was selected as the local patch, which was also used for computing the first order texture features. The threshold slow was set at 0.999 since the pixels are highly similar in terms of the extracted feature vectors.

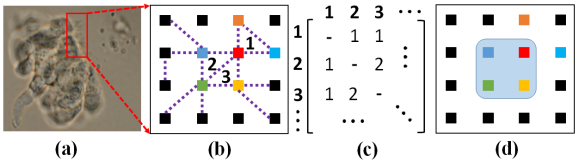


**Fig. 1**. Overview of the region division method. (a) Sample cilia image: the left part is the ciliated cell, right up part is the debris and the cilia are highlighted in red. (b) 3-clique extraction: the neighbourhood relationship between pixels is indicated with the purple lines and the cliques are shown by the triangles with indices. (c) Clique transition matrix: the weights are the numbers of the common pixels between two cliques. (d) Clique propagation: clique 2 and 3 belongs to the same regions.

#### *2.2.2. Clique Identification and Connection*

To divide the different regions, we need to find the pixels that are highly coherent. The direct cosine similarity between pixels is not sufficient to measure the coherence without considering the neighbours. In the proposed method, we use clique as the underlying unit to define how the pixels are related considering the neighbourhood information.

The concept of clique is introduced in graph theory as a subset of vertices such that every two vertices in this subset are connected. In our study, treating the pixel adjacency matrix as a graph, a $k$-clique $C_k$ is a group of $k$ pixels that are neighbouring to each other,

$$\begin{aligned} &C_k = \{p(1), p(2), ..., p(k)\}, \\ &\forall i, j \in [1, k], s.t., pm(p(i), p(j)) = 1 \end{aligned} \quad (2)$$

As shown in Fig.1b, the pixels in a clique (triangle) are fully connected, sharing the common neighbours with each other, thus these pixels are reinforced mutually and are regarded as highly coherent. On the other hand, we have eliminated the unrelated pixels from the surroundings when constructing the neighbourhood hence only the most related pixels are included in a clique.

While the pixels in the same clique are considered to belong to the same class, the next step is to identify how pixels from different cliques are related. We define that two

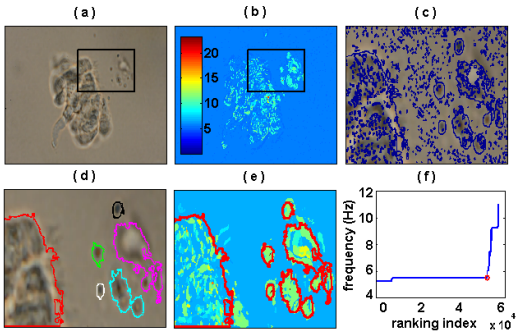


**Fig. 2**. Outline of the CBF estimation: (a) cilia image, (b) frequency map, (c) all regions, (d) foreground and background separation, (e) foreground frequency removal, and (f) frequency distribution. (c) to (e) are from a selected ROI with beating cilia for better visual observation.

cliques are connected if they share common pixels. Supposing there are $h(0 < h < k)$ common pixels, the two cliques are $h$-connected and the pixels in these cliques are related. As shown in Fig.1b, the blue pixel in clique 2 and the yellow pixel in clique 3 are related as the two cliques are 2-connected through the green and red pixels. With this formulation, the pixels are more related if $h$ is higher.

#### *2.2.3. Clique Propagation*

The relationship among all cliques can be represented as a weighted transition matrix $TM$, in which the weight indicates the connectivity according to $h$, i.e., $tm(C(i), C(j)) = h$. Starting from a certain clique, clique propagation is conducted by traversing the whole transition matrix to find the connected cliques. A set of connected cliques then becomes one region of the division result, as shown in Fig.1d. Thresholdings of the weights in the transition matrix are used to control the level of coherence of the connected cliques, as:

$$\begin{cases} tm(C(i), C(J)) = 1, & \textbf{if } h \geq h_{low}, \\ tm(C(i), C(J)) = 0, & \textbf{otherwise} \end{cases} \quad (3)$$

The clique size $k$ and the threshold $h_{low}$ determine the region size. Lowering $k$ and $h_{low}$ will relax the coherence, leading to the larger size regions. In the experiments under study, we selected $h_{low}$ as $k-1$ so that two cliques are highly connected and $k$ was set as 5 that obtained better results in general.

#### *2.2.4. Foreground and Background Separation*

The clique propagation usually results in many regions, most of which are with small sizes, as shown in Fig. 2c. We conduct a filtering process to remove small regions below a certain size $r_{low}$, as shown in Fig.2d. In this way, the cilia regions that are usually with small sizes are merged into the background. In addition, the inside regions that describe the detailed structures of a certain foreground object are linked together to create the overall foreground contours. In the experiments, we set $r_{low}$ as 80, which obtained better separation results across different cases based on our visual observations.

### 2.3. CBF Estimation

CBF is finally measured based on the region division, as illustrated in Fig. 2. Beating frequencies of the foreground regions are removed from the frequency map (Fig. 2e). The frequency distribution is obtained by concatenating the frequencies of all pixels within the background in an ascending order (Fig. 2f). The threshold $t_{low}$ for differentiating the cilia and medium can be easily discovered by finding the breakpoint of the frequency distribution curve[1]. This breakpoint corresponds to the bin of the maximum value in the frequency histogram constructed for all background pixels, since the culture medium pixels occupy the majority of the background and they have the same frequency, as shown with the circle in Fig. 2f. The average (Avg) $\pm$ standard deviation (SD) of the frequencies above $t_{low}$ is used as the CBF estimation in our method.

## 3. EXPERIMENTAL RESULTS AND DISCUSSIONS

Fig.3 shows the CBF estimation results of our proposed method for two cases and their statistics are displayed in Table 1 (cases C1 and C2). The first column in Fig.3 gives the region division results. It can be observed that our method can extract the foreground regions that affect the measurement of CBF, i.e., the cell and debris. Although removing these objects is the first step for our CBF estimation, the identification of them need not be very accurate if we can find the approximate region contours. Therefore, we did not include detailed quantitative evaluations for the region division results.

The second column displays the corresponding region division on frequency map. We can find that the frequencies of the pixels from the cell surface can be very similar to those from the cilia. In addition, the debris can also have similar frequencies with the beating cilia. Thus, identifying the cilia merely based on the frequency spectrum tends to be inaccurate. By incorporating the texture features and the clique propagation method, we can obtain a division result that separates the foreground and background and thus recognize the frequencies of cilia more clearly. In our experiments, the region size $r_{low}$ was empirically set as 80 so that we can include all cilia regions into background, but this also involved some outliers that belong to foreground. The sizes of outliers however were much smaller, which had relatively negligible influence, regarding the whole foreground regions.

[1]The threshold $t_{low}$ is ideally to be 0Hz as the culture medium is still. However, the frequency was calculated with FFT based on the temporal pixel intensity variation that was not constant due to the data acquisition noise. Therefore, $t_{low} > 0$.

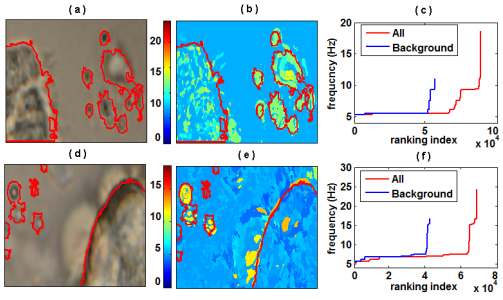


**Fig. 3**. CBF estimation with the proposed method. The first column shows the region division results with foreground regions circled in red. The second column displays the corresponding frequency maps. The third column gives the frequency distributions of the whole frequency map and those obtained by removing the ciliated cell and debris.

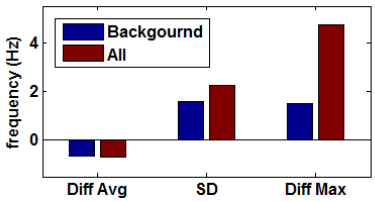


**Fig. 4**. Comparisons between our method (Background) and the control approach (All). The mean differences of Avg and Max (Diff Avg and Diff Max) between the two approaches and the acquisition estimation, and the mean SD of the two approaches are shown here.

The third column shows the frequency distributions of the entire image and the background region. Take the first example for brief explanations, by removing the foreground regions, we can eliminate the frequencies at about 10Hz, which are mainly from debris regions, and the ones between about 12Hz to 20Hz, which are mainly from the inside region of the cell. Based on the threshold scheme (5.03Hz for both cases), the final CBF estimation of these cases is set as $5.73 \pm 0.93$Hz and $7.07 \pm 1.71$Hz with the maximum 11.00Hz and 16.62Hz through our proposed method.

We reported the detailed CBF estimation statistics on some other cases in Table 1. To illustrate that our CBF estimation is reasonable, we provided the acquisition estimation (Acq) during the acquisition process with a Zeiss photomultiplier, where the electronic signals from the photometer were delivered through an oscilloscope and subsequently recorded by Mac-Lab recording system. Our method (Bac) obtained a CBF close to the acquisition estimation, measured by Avg $\pm$ SD, showing that the proposed method can describe the ciliary motility properly. The overall comparisons across the 30 cases between our method and the approach (All) that did not remove the foreground regions are displayed in Fig.4. Our method provided similar average CBF to the control approach, both of which had lower mean Avg than the acquisition estimation across the 30 cases. However, we obtained a smaller SD by measuring the CBF in a more compact range. In addition, the proposed method can help to reduce the influence by the high frequencies from the foreground regions so that our maximum CBF was closer to the acquisition estimation compared to the control approach.

**Table 1**. CBF estimation statistics

| CI & Con | | Avg(Hz) | SD(Hz) | Max(Hz) |
|---|---|---|---|---|
| C1 | Acq | 4.51 | 0.96 | 7.00 |
| SS:$10^{-8}$M | All | 6.20 | 1.50 | 18.61 |
| | Bac | **5.73** | **0.93** | **11.00** |
| C2 | Acq | 9.78 | 1.92 | 16.00 |
| MA:$10^{-3}$M | All | 7.24 | 2.20 | 24.23 |
| | Bac | **7.07** | **1.71** | **16.62** |
| C3 | Acq | 5.43 | 0.52 | 7.00 |
| SS:$10^{-7}$M | All | 6.45 | 1.02 | 12.64 |
| | Bac | **6.42** | **0.96** | **11.71** |
| C4 | Acq | 8.73 | 1.64 | 12.00 |
| SS: $2 \cdot 10^{-3}$M | All | 9.47 | 1.87 | 11.47 |
| MA: $10^{-3}$M | Bac | **9.57** | **1.27** | **11.47** |
| C5 | Acq | 9.95 | 1.66 | 15.00 |
| No drug | All | 9.44 | 2.36 | 22.95 |
| | Bac | **10.00** | **1.48** | **12.29** |

*CI: case index, Con: concentration, M: molarity, Avg: average, SD: standard deviation, Max: maximum.

## 4. CONCLUSIONS AND FUTURE WORK

An image-based CBF estimation method is presented for describing the ciliary beating behaviors, by removing the unfavorable objects that can affect observing the cilia. Focusing on the cilia region only, the proposed method is expected to be suitable for finding the defective ciliary motility and observing the therapeutic effects of different drugs. The most significant change with our method can be observed by a closer maximum CBF to the acquisition estimation. Compared to the whole field analysis, our method provides a substantial improvement since the maximum frequencies are normally used to describe the most active ciliary motion.

In our future work, we will conduct more comprehensive evaluations, including the influence of different parameter settings and the quantitative comparison of foreground region division results. The more advanced methods from the computer vision, such as object detection and segmentation, are expected to improve foreground removal and will be incorporated in our CBF measurement method. While the preliminary experimental results have shown promising performance of our method, we will further investigate its practicability based on more clinical studies of healthy and dysfunctional beating patterns.

## 5. ACKNOWLEDGEMENT

This work was supported in part by ARC grants.

## 6. REFERENCES


[1] J. H. Sisson, J. A. Stoner, B. A. Ammons, and T. A. Wyatt, "All-digital image capture and whole-field analysis of ciliary beat frequency," *Journal of Microscopy*, vol. 211, no. 2, pp. 103–111, 2003.

[2] M. A. Chilvers, A. Rutman, and C. O'Callaghan, "Ciliary beat pattern is associated with specific ultrastructural defects in primary ciliary dyskinesia," *Journal of Allergy and Clinical Immunology*, vol. 112, no. 3, pp. 518–524, 2003.

[3] M. Salathe and R. J. Bookman, "Mode of ca2+ action on ciliary beat frequency in single ovine airway epithelial cells," *The Journal of Physiology*, vol. 520, no. 3, pp. 851–865, 1999.

[4] G. Mantovani, M. Pifferi, and G. Vozzi, "Automated software for analysis of ciliary beat frequency and metachronal wave orientation in primary ciliary dyskinesia," *European Archives of Oto-Rhino-Laryngology*, vol. 267, no. 6, pp. 897–902, 2010.

[5] J. Yager, T. Chen, and M. J. Dulfano, "Measurement of frequency of ciliary beats of human respiratory epithelium," *CHEST Journal*, vol. 73, no. 5, pp. 627–633, 1978.

[6] H. Teichtahl, P. L. Wright, and R. L. G. Kirsner, "Measurement of in vitro ciliary beat frequency: a television-video modification of the transmitted light technique," *Medical and Biological Engineering and Computing*, vol. 24, no. 2, pp. 193–196, 1986.

[7] W. Kim, T. H. Han, H. J. Kim, M. Y. Park, K. S. Kim, and R. W. Park, "An automated measurement of ciliary beating frequency using a combined optical flow and peak detection," *Healthcare Informatics Research*, vol. 17, no. 2, pp. 111–119, 2011.

[8] M. A. Chilvers, A. Rutman, and C. O'Callaghan, "Ciliary beat pattern is associated with specific ultrastructural defects in primary ciliary dyskinesia," *Journal of Allergy and Clinical Immunology*, vol. 112, no. 3, pp. 518–524, 2003.

[9] C. O'Callaghan, K. Sikand, and M. A. Chilvers, "Analysis of ependymal ciliary beat pattern and beat frequency using high speed imaging: comparison with the photomultiplier and photodiode methods," *Cilia*, vol. 1, no. 8, pp. 1–7, 2012.

[10] D. Koniar, L. Hargas, and M. Hrianka, "Measurement of object beating frequency using image analysis," in *Applied Electronics*, 2009, pp. 153–156.

[11] C. M. Smith, J. Djakow, R. C. Free, P. Djakow, R. Lonnen, G. Williams, P. Pohunek, R. A. Hirst, A. J. Easton, and P. W. Andrew, "ciliafa: a research tool for automated, high-throughput measurement of ciliary beat frequency using freely available software," *Cilia*, vol. 1, no. 14, pp. 1–7, 2012.

[12] D. Koniar, L. Hargaš, and S. Štofan, "Segmentation of motion regions for biomechanical systems," *Procedia Engineering*, vol. 48, pp. 304–311, 2012.

[13] E. Parrilla, M. Armengot, M. Mata, J. Cortijo, J. Riera, J. L. Hueso, and D. Moratal, "Optical flow method in phase-contrast microscopy images for the diagnosis of primary ciliary dyskinesia through measurement of ciliary beat frequency. preliminary results," in *IEEE International Symposium on Biomedical Imaging (ISBI)*, 2012, pp. 1655–1658.

[14] F. Zhang, W. Cai, Y. Song, P. Young, D. Traini, L. Morgan, H. Ong, L. Buddle, and D. Feng, "Image-based ciliary beating frequency estimation for therapeutic assessment on defective mucociliary clearance diseases," in *IEEE International Symposium on Biomedical Imaging (ISBI)*, 2014, pp. 193–196.